Decentralized Multi-Agent System-Based Cooperative Frequency Control for Autonomous Microgrids With Communication Constraints

Wei Liu, *Student Member*, *IEEE*, Wei Gu, *Member*, *IEEE*, Wanxing Sheng, *Member*, *IEEE*, Xiaoli Meng, *Member*, *IEEE*, Zaijun Wu, *Member*, *IEEE*, and Wu Chen, *Member*, *IEEE*

***Abstract*—Based on power line carrier communication technology, a decentralized multi-agent system (DMAS)-based frequency control strategy is proposed and investigated in this study on an autonomous microgrid with communication constraints, where each agent can only communicate with its neighboring agents. Using the optimized average consensus algorithm, the global information (i.e., total active power deficiency of the microgrid) can be accurately shared in a decentralized way. Depending on the discovered global information, the cooperative frequency control strategy, which involves primary and secondary frequency control and multi-stage load shedding, is executed to achieve a cooperative frequency recovery. Simulation results indicate that the proposed frequency control approach can guarantee the consensus and coordination of the distributed agents and maintain the frequency stability of islanded microgrids even in emergency conditions.**

***Index Terms*—Average consensus algorithm (ACA), cooperative frequency control, decentralized multi-agent system (DMAS), global information, multi-stage load shedding (LS).**

I. Introduction

FREQUENCY control of an autonomous microgrid is achieved by coordinating the energy storage (ES), such as superconducting magnetic energy storage (SMES) and battery energy storage (BES), available distributed generators (DGs), such as wind turbines (WTs), photovoltaics (PVs), and microturbines (MTs), and controllable loads. An autonomous microgrid is an isolated power system with a small equivalent inertia, which makes its frequency control more difficult than conventional power systems. Because of the operation mode, transfer and intermittent characteristics of some distributed generators, frequency deviation caused by active power deficiency or shortage often occurs in an islanded microgrid [1], [2]. As a result, the frequency of the microgrid will fluctuate and may change rapidly due to the low inertia present and even experience a blackout unless there is adequate available spinning reserve to balance it [3], [4].

To overcome this limitation previously, local control strategy of ESs was introduced and considered a solution for frequency stabilization of an islanded microgrid. ESs can absorb or inject instantaneous power to provide support for primary frequency control [5]. Subsequently, it was recognized that the power distribution of DGs can also play an important role in maintaining the frequency stability and regulating the microgrid to a new balanced state [6], [7]. It has to be noted that the WTs, which mainly imply double fed induction generators (DFIGs), operate in a reserve power mode and can effectively provide support for the system frequency using auxiliary frequency control [8]–[10]. A two-layered hierarchical frequency control scheme with microgrid central control (MGCC) was proposed to achieve cooperative frequency recovery by coordinating the ESs and DGs [11], [12]. Eventually, a multi-agent system (MAS) was presented as one of the effective solutions for the decentralized frequency control of a microgrid [13].

Similar to two-layered hierarchical frequency control, the corresponding centralized multi-agent system (CMAS) also requires a powerful MGCC [13], [14], which is expensive and can easily suffer failures when handling huge amounts of data. In addition, a CMAS lacks the adaptability to meet the plug-and-play operation requirements of a microgrid. Furthermore, taking the uncertainty of intermittent renewable energy resources into consideration, generation fluctuation may result in unintentional changes in structure, which will further increase the burden on centralized schemes. In contrast, because of the limitations of communication technology, the communication between the MGCC agent and local agents is difficult to guarantee [15], [16].

This study introduces a decentralized multi-agent system (DMAS) without an MGCC for frequency control of an autonomous microgrid to overcome the above-mentioned shortcomings. The advantages of DMAS include the ability to survive uncertainty disturbances and decentralized data updating, which leads to efficient information sharing, eventually causing a faster decision-making process and operation [16], [17]. The ACA, which relies on local information from the agents and solves the consensus problems of DMAS, was introduced by Olfati-Saber and Murray in [18]. Further theoretical extensions of this work were presented in [19]–[22] and a recent survey can be found in [23].

Recently, MAS and the corresponding consensus algorithm have found applications in various areas, such as random networks, multi-robot systems, and power grids. In [24], a stable

Manuscript received April 28, 2013; revised July 29, 2013 and October 19, 2013; accepted November 24, 2013. Date of publication January 10, 2014; date of current version March 18, 2014. This work was supported in part by the National High Technology Research and Development Program of China (863 Program Grant 2011AA05A107), in part by the National Science Foundation of China (Grant 51277027), in part by the Natural Science Foundation of Jiangsu Province of China (Grant SBK201122387), and in part by the Fundamental Research Funds for the Central Universities.

W. Liu, W. Gu, Z. Wu, and W. Chen are with the School of Electrical Engineering, Southeast University, Nanjing, Jiangsu 210096, China (e-mail: wgu@seu.edu.cn).

W. Sheng and X. Meng are with the Power Distribution Department, China Electrical Power Research Institute, Beijing 100192, China.

Color versions of one or more of the figures in this paper are available online at http://ieeexplore.ieee.org.

Digital Object Identifier 10.1109/TSTE.2013.2293148

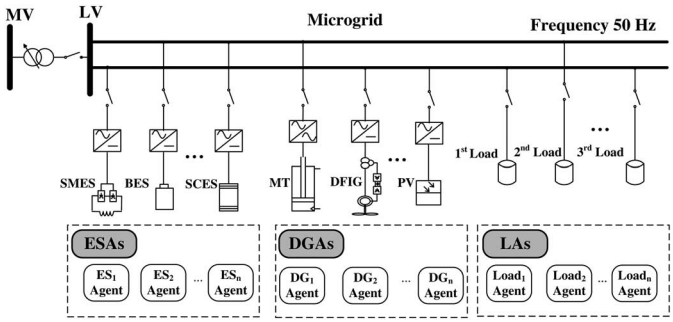

Fig. 1. DMAS-based frequency control framework.

multi-agent-based load shedding (LS) algorithm for power systems was proposed and verified. An incremental cost consensus algorithm under different communication network topologies in a smart grid was studied and the convergence of the proposed algorithm was analyzed in [25]. An MAS-based scheme for a microgrid was presented in [26] to secure critical loads for a PV-based microgrid, and a centralized MAS-based frequency control method was proposed and investigated in [13] to enhance the frequency stability of an islanded microgrid. Accordingly, in this study, an optimized average consensus algorithm (ACA) is proposed to guarantee that important information is shared in a distributed way for a DMAS with communication constraints, where an agent can only communicate with immediate neighboring agents. In addition, the impacts of communication time delays and adaption of topology changes are further discussed in this paper.

Depending on the optimized ACA-based information sharing, a two-layered cooperative control structure can be used for the proposed strategy: 1) the primary control action in ESs and 2) the secondary control actions in DGs. The control structure regulates the power output of the ESs to the initial state. To evaluate the proposed control strategy, a simulation system was designed and the corresponding dynamic simulation model based on PSCAD/EMTDC was developed. Both the optimized ACA and cooperative frequency control were realized using the PSCAD/EMTDC and MATLAB interface technologies. Simulation results are presented and discussed to illustrate the dynamic performance of the proposed control strategy.

The rest of the paper is organized as follows. Section II gives a brief introduction on DMAS-based frequency control of an islanded microgrid. In Section III, the optimized ACA-based information sharing of DMAS is proposed. Section IV presents the DMAS-based cooperative frequency control method. The proposed method is then simulated and illustrated with a simulation system in Section V. Finally, the conclusion is duly drawn.

II. Background

In order to achieve a decentralized frequency control for an islanded microgrid without an MGCC, it has to confront the following difficulties: 1) how to control each distributed unit locally; 2) how to coordinate the different kinds of distributed units (including DGs, ESs, and multi-stage loads) and realize a cooperative control in a decentralized manner; and 3) how to meet the plug-and-play operations of a microgrid. It is hard to deal with these problems by traditional control schemes, and thus the MAS-based control is proposed to solve the special needs and difficulties above. There are advantages for introducing the MAS for frequency control of an islanded microgrid.

1) Autonomy of agents is appropriate to deal with the independent decision making of distributed units.
2) Intelligence and sociality of agents can properly handle the communication and cooperation among groups of distributed units.
3) Proactivity and adaptability of agents can adequately adapt to the dynamic changes of communication topologies and the plug-and-play operations of distributed units.

In this study, a DMAS-based frequency control framework without an MGCC is proposed to implement cooperative control of DGs, ESs, and loads of an autonomous microgrid, as shown in Fig. 1. For the DMAS, each DG, ES, and load corresponds to a distributed agent and taking advantage of the autonomous, intelligent, cooperative, proactive, and adaptive features of the DMAS, the frequency stability of the microgrid can be guaranteed by coordinating these decentralized agents.

Agents of DMAS include the distributed generation agent (DGA), energy storage agent (ESA), and load agent (LA). In the DMAS, DGAs, ESAs, and LAs are allocated to improve the frequency stability of the autonomous microgrid. Compared with the CMAS, which coordinates its local agents using an MGCC, in the DMAS, the distributed agents are coordinated based on the discovered global information, such as total active power deficiency, total available active power, and operating status of loads. This global information can be discovered only by communication between the immediate neighboring agents according to the designed ACA. Consequently, the control modes and corresponding decision making for each agent can be determined.

III. Optimized ACA-Based Information Sharing

It has to be noted that, if there is limited local or incomplete information in a DMAS, it is hard to ensure the consensus of target performance and behavior between the decentralized agents. Therefore, the ACA, which relies on the local information of agents, is applied to guarantee the important global information and is shared in a distributed way. In this study, a discrete form of the ACA is chosen to achieve global information on the active power in the DMAS with communication constraints [23], [25]. Thus, based on the ACA, power information sharing can be solved in a decentralized manner instead of in a conventional centralized manner in a DMAS.

Assume that $p_i \in R$ denotes the state variable (active power) of agent i. The information sharing process for agent i with time delay can be represented as

$$p_i^{[k+1]}(t+\tau_{ij}) = p_i^{[k]}(t) + \sum_{j\in N_i} w_{ij} p_j^{[k]}(t) \tag{1}$$

where $i = 1, 2, \ldots, n$, $j = 1, 2, \ldots, n$; k is the discrete-time index; $p_i^{[k]}$ and $p_i^{[k+1]}$ are the information shared by agent i at iteration k and $k+1$, respectively, $p_j^{[k]}$ is the information sharing of agent j; τ_{ij} is the time delay; w_{ij} is the coefficient for information exchange between neighboring agents i and j, if agents i and j are connected through a communication line, otherwise $w_{ij} = 0$, and N_i are the indexes of agents that are

connected to a specific agent. The global information sharing process of the microgrid can be represented using a matrix format as

$$\begin{cases} \boldsymbol{P}^{[k+1]}(t+\Gamma) = \boldsymbol{W} * \boldsymbol{P}^{[k]}(t) \\ \Gamma = \Gamma_{\text{cal}} + \Gamma_{\text{com}} = \Gamma_{\text{cal}} + \frac{n_{\text{bit}}}{V_{\text{com}}} * (n_e * n_P) \end{cases} \tag{2}$$

where $\boldsymbol{P}^{[k]}$ is the information sharing matrix; $\boldsymbol{W}$ is the updating matrix, which can be defined according to the communication topology; Γ is the time delay of information sharing in one iteration process; Γ_{cal} is the calculation time delay and Γ_{com} is the communication time delay; n_e is the number of the information exchange times; n_P is the number of elements in the information sharing matrix; n_{bit} is the number of bits used to represent the elements in the information sharing matrix; and V_{com} is the data communication speed in terms of bits/second. For such an information exchange topology, which is strongly connected and balanced, this $\boldsymbol{W}$ satisfies the following constraints:

$$\begin{cases} \sum\limits_i w_{ij} = 1 \\ \sum\limits_j w_{ij} = 1. \end{cases} \tag{3}$$

To obtain a stable algorithm, the updating rule or the coefficients need to be properly designed. To adapt to changes in system configuration, a *Metropolis* method was presented in [16] and [17], as follows:

$$w_{ij} = \begin{cases} 1/[\max(n_i + n_j) + 1], & j \in N_i \\ 1 - \sum\limits_{j \in N_i} 1/[\max(n_i + n_j) + 1], & j = i \\ 0, & \text{otherwise.} \end{cases} \tag{4}$$

In this study, an optimized *Metropolis* method is proposed to improve the converging speed and the corresponding adaptive weights updating rule is represented as

$$w_{ij} = \begin{cases} \theta/[(n_i + n_j)/2], & j \in N_i \\ 1 - \sum\limits_{j \in N_i} \theta/[(n_i + n_j)/2], & j = i \\ 0, & \text{otherwise} \end{cases} \tag{5}$$

where θ is a constant, $0 < \theta < 1$, and θ is in close proximity to 1, n_i and n_j are the numbers of agents in the neighborhood of agents i and j, respectively. For stability analysis, a positive definite *Lyapunov* function can be defined as

$$\begin{aligned} &L = (\boldsymbol{P}^{[k]})^T, \quad \boldsymbol{P}^{[k]} w_{ij} = \frac{\theta}{(n_i + n_j)/2}, \quad i \neq j \\ &\Delta L = [(\boldsymbol{P}^{[k]})^T (\boldsymbol{W}^T \boldsymbol{W} - \boldsymbol{I}) \boldsymbol{P}^{[k]}] \\ &\quad \le -\sum_{i=1}^{n} \sum_{j=1}^{n} [(w_{ij} + w_{ij}^2)(p_j^{[k]} - p_i^{[k]})^2] \\ &\quad + \frac{1}{2} \sum_{i=1}^{n} \sum_{j=1}^{n} [(n_i + n_j - 2) w_{ij}^2 (p_j^{[k]} - p_i^{[k]})^2] \\ &\quad \le -\sum_{i=1}^{n} \sum_{j=1}^{n} \left[\left(\frac{2 - (n_i + n_j) w_{ij}}{2} \right) w_{ij} (p_j^{[k]} - p_i^{[k]})^2 \right] \\ &\quad \le -\sum_{i=1}^{n} \sum_{j=1}^{n} \left[\frac{\theta(1-\theta)}{n_i + n_j} (p_j^{[k]} - p_i^{[k]})^2 \right] \\ &0 < \theta < 1 \Rightarrow \Delta L \le 0. \end{aligned} \tag{6}$$

From the verification, it is obvious that the proposed optimized *Metropolis* method can guarantee stability during the information sharing process. Depending on the proposed method, an agent can adjust its coefficients locally to adapt to changes in the system configuration, such as plug-and-play operations of switching topology.

Based on the stability analysis, every agent needs to update its value p_i to a certain weighted linear combination of its neighbors' values, and p_i will converge to the same value, as follows:

$$\begin{cases} P_{\text{AVE}} = \sum\limits_i p_i^{[0]}/n \Rightarrow P_{\text{AVE}}^{\text{TOT}} = n * P_{\text{AVE}} \\ \Gamma^{\text{TOT}} = n_c * \Gamma \end{cases} \tag{7}$$

where P_{AVE} is the final average power achieved by the ACA-based information sharing, $P_{\text{TOT}}^{\text{AVE}}$ is the total power, $p_i^{[0]}$ is the initial value of the ith agent, n is the total number of agents that participate in global information sharing, and n_c is the number of iterations for convergence. Assuming that the time delays of all the iterations are the same, the total time delay Γ^{TOT} can be estimated from (7).

IV. DMAS-Based Cooperative Frequency control

The frequency control of an islanded microgrid includes the primary and secondary frequency controls as in the conventional power systems. The objective of primary frequency control is to maintain the frequency stability of the microgrid quickly and automatically using the power stored in the ESAs. Two objectives ranked in the secondary frequency control are designed through the power output control of the DGAs. One is to regulate the frequency to a rated value and the other is to recharge the ESs to increase the reserve power for dealing with emergencies.

In this study, it is assumed that every bus in the microgrid is assigned with an agent to form the DMAS. According to the two-layer frequency control strategy, in the first layer, the ESAs enable primary frequency control to happen automatically without the need of interaction between the agents. Ranked in the secondary frequency control, the DGAs adjust the power outputs of the DGs until the microgrid reaches a new steady state. Therefore, each agent evaluates its corresponding distributed unit and makes the classification according to its relative participation during the frequency control. Universally, the controllers of inverters in the ESs respond in milliseconds. Otherwise, the MT and WT have a relatively slower response time. Accordingly, the distributed units of the microgrid can be classified into several levels. Related to the DMAS-based cooperative control structure, the ESAs act on primary frequency control; whereas the DGAs act on secondary frequency control and regulate the power outputs of the ESs to zero, and the multi-stage LS in the LAs is used as a standby source to ensure the effect of the secondary control. Therefore, in this study, the ESAs are defined as the first level, the DGAs belong to the second level, and the LAs are in the third level. Detailed classification of distributed agents is described in Table I.

Every agent knows its corresponding local power outputs and load conditions, but does not have direct access to the global

TABLE I
CLASSIFICATION OF DISTRIBUTED AGENTS OF MICROGRID

Frequency control	Agent	Level
Primary	ESA	1
Secondary	DGA	2
	LA	3

information. It can only communicate with its immediate neighboring agents, which are connected to it through electrical lines. Thus, the main challenge in the design of a DMAS-based frequency control strategy is to discover the global information through information exchange between the decentralized agents. This can be resolved by the proposed optimized ACA-based information sharing detailed in Section III. The global information, such as the total power deficiency, total available power, and indexes of multi-stage loads can be discovered from the decentralized agents.

Fig. 2 illustrates the flowchart of the DMAS-based cooperative frequency control strategy. The corresponding steps for the two-layer cooperative control of active power deficiency sharing and distribution can be described as follows:

Step 1) Each agent evaluates its response time for the distributed unit and makes the classification according to its relative participation during the frequency control. The primary frequency control occurs automatically in the ESAs, so that the total power output changes of the ESs can be regarded as the total active power deficiency $P_{\mathrm{DEF}}^{\mathrm{TOT}}$ of the microgrid (assume that the initial states of the ESs are zero) [12], which is shared in the DMAS based on ACA, as $n * P_{\mathrm{DEF}}$ in (8).

Step 2) Ranked as second, with regard to the DGs action in secondary frequency control, the total available power $P_{\mathrm{AVA}}^{\mathrm{TOT}}$ is estimated and shared by the optimized ACA-based information sharing method, to all decentralized agents as $n * P_{\mathrm{AVA}}$, as described in (8).

Step 3) In this step, the total power deficiency $P_{\mathrm{DEF}}^{\mathrm{TOT}}$ and the available power $P_{\mathrm{AVA}}^{\mathrm{TOT}}$ achieved by the ACA information discovery method are compared, and if $P_{\mathrm{DEF}}^{\mathrm{TOT}} \le P_{\mathrm{AVA}}^{\mathrm{TOT}}$, then the power deficiency will be made up by the power increasing for the DGs in the proportion of $P_{\mathrm{DEF}}^{\mathrm{TOT}}/P_{\mathrm{AVA}}^{\mathrm{TOT}}$, as in (9).

Step 4) Related to the discussion above, if $P_{\mathrm{DEF}}^{\mathrm{TOT}} > P_{\mathrm{AVA}}^{\mathrm{TOT}}$, it is necessary to implement LS because the reserve power in the DGs is not enough to make up the power deficiency, and the amount of load to be shed can be derived by $P_{\mathrm{LS}}^{\mathrm{TOT}} = P_{\mathrm{DEF}}^{\mathrm{TOT}} - P_{\mathrm{AVA}}^{\mathrm{TOT}}$, as in (10).

Step 5) Finally, the multi-stage LS approach is implemented to make up the power deficiency and the amounts of load for each LA are described in (11).

A. Information Sharing for Microgrid

When a power disturbance occurs in the autonomous microgrid, the global information for cooperative frequency control of the DMAS includes the total number of agents that participate in global information sharing n, the total power deficiency $P_{\mathrm{DEF}}^{\mathrm{TOT}}$, and the available power $P_{\mathrm{AVA}}^{\mathrm{TOT}}$ and these are shared among the decentralized agents. The proposed ACA-based information sharing method is used to calculate global information indirectly. If (1) is initialized with the predefined index i of the ith agent, it will converge to the average i/n through information sharing, thus the number n can be easily determined as $i/(i/n)$. Similarly, if (1) is initialized with active power changes of the ESs, it will converge to the average of total power deficiency after information sharing, which is represented as P_{DEF}. The total power deficiency $P_{\mathrm{DEF}}^{\mathrm{TOT}}$ can be obtained by multiplying P_{DEF} by n. The process of the global information sharing can be expressed as

$$\begin{cases} P_{ai} = i/n \Rightarrow n = i/(i/n) \\ P_{\mathrm{DEF}} = \sum_x \Delta P_{\mathrm{ES}x}^{[0]}/n \\ \qquad x = 1,2,\ldots,n \qquad \Rightarrow \begin{cases} P_{\mathrm{DEF}}^{\mathrm{TOT}} = n * P_{\mathrm{DEF}} \\ P_{\mathrm{AVA}}^{\mathrm{TOT}} = n * P_{\mathrm{AVA}} \end{cases} \\ P_{\mathrm{AVA}} = \sum_y \Delta P_{\mathrm{DG}y}^{[0]}/n \\ \qquad = \sum_y (P_{\mathrm{DG}y}^{\mathrm{Max}[0]} - P_{\mathrm{DG}y}^{[0]})/n \\ \qquad y = 1,2,\ldots,n \end{cases} \tag{8}$$

where $\Delta P_{\mathrm{ES}x}^{[0]}$ is the active power output change of the xth ES unit in its initial state, $\Delta P_{\mathrm{DG}y}^{[0]}$ is the maximum available active power of the yth DG unit in its initial state, $P_{\mathrm{DG}y}^{\mathrm{Max}[0]}$ is the maximum active power capacity of the yth DG unit, and $P_{\mathrm{DG}y}^{[0]}$ is the active power of the yth DG unit in its initial state.

To meet the plug-and-play operation requirements for a DMAS-based microgrid, an identity (ID) updating method for the agent is used for the ACA-based information sharing. If a new agent is added, the corresponding new agent will require a unique ID to interact with the existing agents, and during the plug-in operation only local information needs to be updated. Because $n+1$ agents participate in information sharing, the index of the ith agent will converge to $i/(n+1)$ instead of i/n as in (8), so the new agent will determine its ID as being $n+1$ according to the converged average value. With respect to the plug-out operation, the IDs of the existing agents do not need to be updated during the information sharing. However, special attention is required during long-term or permanent changes to the network topology. If an existing agent is permanently removed, IDs of remaining agents may need to be updated to simplify the ID acquisition of new agents.

B. Cooperative Power Distribution

In the primary frequency control, the ESAs automatically control the ESs to make up the power deficiency immediately after a disturbance, while in the secondary frequency control, the DGAs increase the available power of the DGs and regulate the power outputs of the ESs to zero. In Section IV-A, $P_{\mathrm{DEF}}^{\mathrm{TOT}}$ and $P_{\mathrm{AVA}}^{\mathrm{TOT}}$ are achieved and shared by ACA to all decentralized agents. Different power distribution strategies will be carried out based on the comparison of $P_{\mathrm{DEF}}^{\mathrm{TOT}}$ with $P_{\mathrm{AVA}}^{\mathrm{TOT}}$.

1) If $P_{\mathrm{DEF}}^{\mathrm{TOT}} \le P_{\mathrm{AVA}}^{\mathrm{TOT}}$, then the power deficiency is offset by the DGs which have available power or reserve power, and

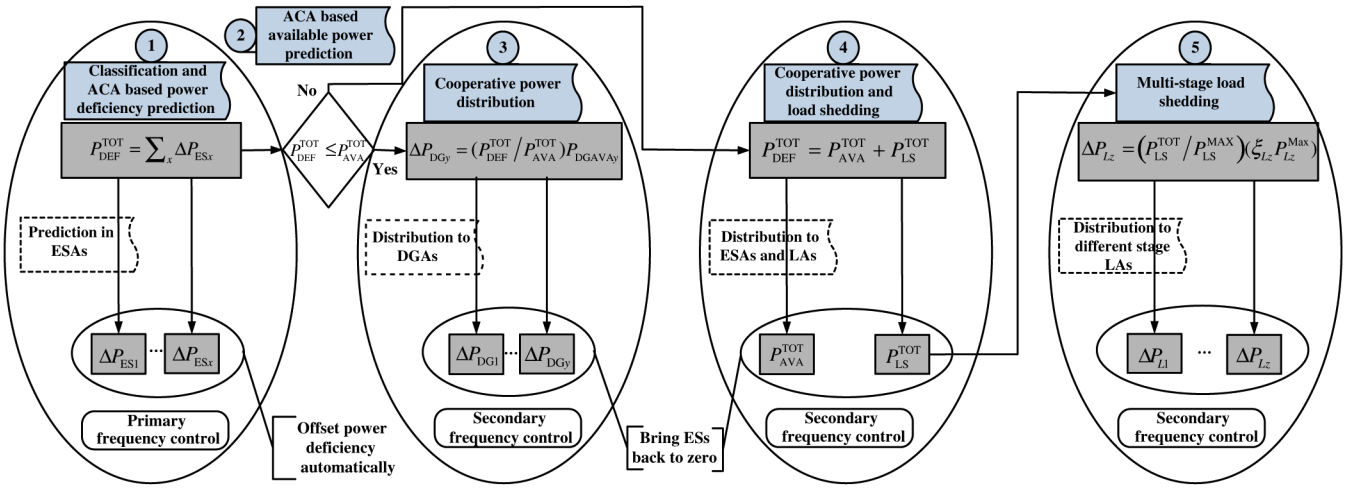

Fig. 2. Flowchart of cooperative frequency control for islanded microgrid.

each DGA increases its corresponding power in proportion to $P_{\mathrm{DEF}}^{\mathrm{TOT}}/P_{\mathrm{AVA}}^{\mathrm{TOT}}$

$$\Delta P_{\mathrm{DG}y}=(P_{\mathrm{DEF}}^{\mathrm{TOT}}/P_{\mathrm{AVA}}^{\mathrm{TOT}})*\Delta P_{\mathrm{DG}y}^{[0]},\quad y=1,2,\ldots,n. \tag{9}$$

2) If $P_{\mathrm{DEF}}^{\mathrm{TOT}}>P_{\mathrm{AVA}}^{\mathrm{TOT}}$, then the LS strategy must be implemented because the reserve power in the DGs is not enough to make up the power deficiency. The load to be shed is $P_{\mathrm{DEF}}^{\mathrm{TOT}}-P_{\mathrm{AVA}}^{\mathrm{TOT}}$

$$\begin{cases}\Delta P_{\mathrm{DG}y}=P_{\mathrm{DG}y}^{\mathrm{Max}}-P_{\mathrm{DG}y},\quad y=1,2,\ldots,n\\ P_{\mathrm{DEF}}^{\mathrm{TOT}}=P_{\mathrm{AVA}}^{\mathrm{TOT}}+P_{\mathrm{LS}}^{\mathrm{TOT}}.\end{cases} \tag{10}$$

C. Multi-Stage LS

First, taking advantage of the optimized ACA, the other global information $P_{\mathrm{LS}}^{\mathrm{MAX}}$ (maximum capacity of load) is shared to all the decentralized agents as $P_{\mathrm{DEF}}^{\mathrm{TOT}}$ and $P_{\mathrm{AVA}}^{\mathrm{TOT}}$, as in Section IV-A. Multi-stage LS is implemented based on the discovered information $P_{\mathrm{LS}}^{\mathrm{MAX}}$ and the power deficiency is made up as $P_{\mathrm{LS}}^{\mathrm{TOT}}$. The information sharing process and the loads to be shed can be derived as follows:

$$\begin{cases}P_{\mathrm{LS}}=\sum\limits_z \xi_{Lz}P_{Lz}^{\mathrm{Max}}/n\Rightarrow P_{\mathrm{LS}}^{\mathrm{MAX}}=n*P_{\mathrm{LS}}\\ \Delta P_{Lz}=(P_{\mathrm{LS}}^{\mathrm{TOT}}/P_{\mathrm{LS}}^{\mathrm{MAX}})*(\xi_{Lz}P_{Lz}^{\mathrm{Max}}) \qquad z=1,2,\ldots,n\\ \qquad\quad =[(P_{\mathrm{DEF}}^{\mathrm{TOT}}-P_{\mathrm{AVA}}^{\mathrm{TOT}})/P_{\mathrm{LS}}^{\mathrm{MAX}}]*(\xi_{Lz}P_{Lz}^{\mathrm{Max}})\end{cases} \tag{11}$$

where z is the zth load unit, $z=1,2,\ldots$; P_{Lz}^{Max} is the maximum capacity limitation of the zth load, ΔP_{Lz} is the load to be shed for the zth load unit; and ξ_{Lz} is the participation coefficient of the zth load, which is achieved based on the stages of the loads. Note that the loads can be divided into three stages according to political and economic influences caused by load interruption. The first stage load is the uninterruptible power supplied vital load, interruption of which would cause great political reaction and economic losses, and even human casualties; interruption of the second stage load would cause certain political reaction and economic loss; and the third stage load is the nonvital adjustable load [14]. The proposed multi-stage LS takes the load stages into consideration, which can achieve frequency restoration mainly by adjustable LS and ensuring an uninterruptible power supply in the most important loads.

V. Simulation Results

To test the effectiveness of the proposed approach, a simulated microgrid on PSCAD/EMTDC was developed. The simulated microgrid is an isolated self-governing microgrid, and the configuration of the simulated microgrid used in this study is shown in Fig. 3. It is composed of a 0.38-kV distributed subsystem connected to a 10-kV distribution network through a 100-kVA transformer. The MT operates in the voltage (V) and frequency (F) control (VF control) mode and other DERs operate in the active power (P) and reactive power (Q) control (PQ control) mode. The total capacity of DERs is 135 kW, including 65 kW of MT, 40 kW of WT (DFIG), 10 kW of PV, 20 kW of BES_1, and 15 kW of BES_2. The total loads are 10 kW of first stage loads, 48 kW of second stage loads, and 77 kW of third stage loads. It has to be noted that the total loss of the lines in the distribution network and loss of the operation process are neglected for simplification and convenience of simulation.

PSCAD/EMTDC and MATLAB interface technologies are used to model the DMAS-based microgrid. More specifically, the microgrid is modeled in PSCAD, whereas the agents are simulated in MATLAB, and user-defined interface (UDI) models in PSCAD are designed to link these two platforms. Through these interface models, the agents in MATLAB can collect data from PSCAD and send the control reference values back to PSCAD for decentralized control after ACA-based information sharing in MATLAB, as shown in Figs. 4 and 5. The communication time delay is estimated mainly based on the data size, communication speed, and convergence times, as described by (2) and (7).

As can be seen from Figs. 4 and 5, the UDI models in PSCAD can implement the interaction among the agents and controllable devices, and through these interface models, the data in PSCAD, such as the agent index, number of neighbors, active power

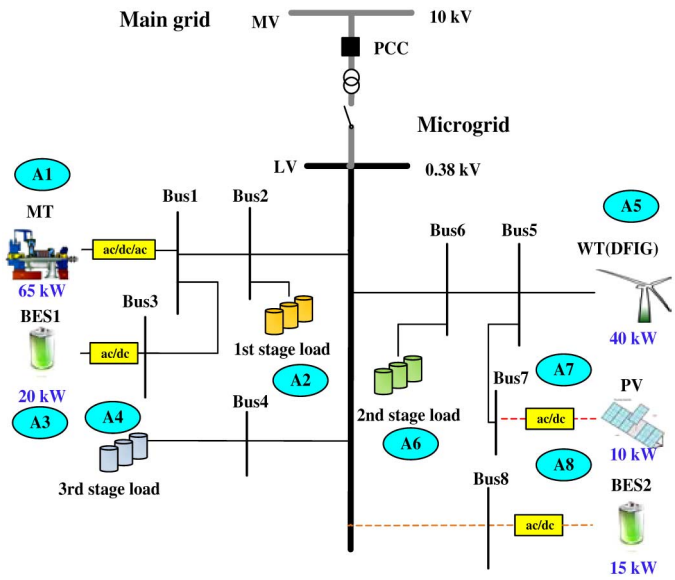

Fig. 3. Microgrid architecture.

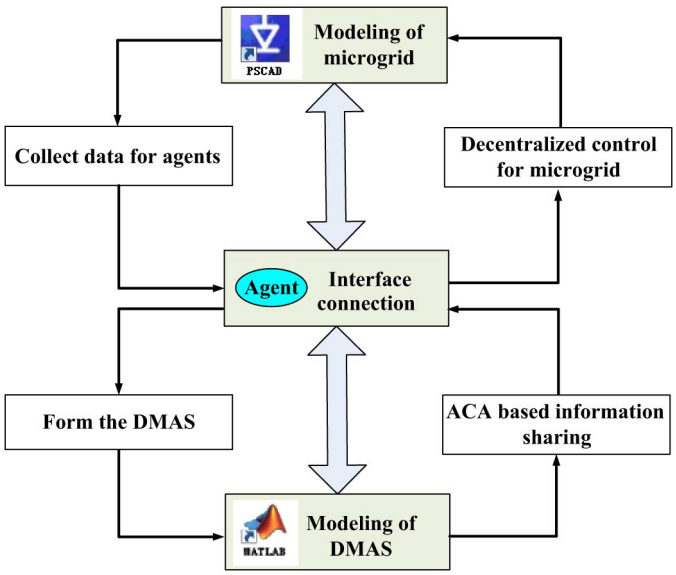

Fig. 4. Flowchart of modeling with PSCAD and MATLAB.

outputs of the agent and its neighbors, and system frequency can be collected in MATLAB. The agents modeled in MATLAB can then exchange data with their neighbors and discover the global information using the ACA in a distributed manner. After information sharing, the control reference values are passed from the agents to the devices in PSCAD for decentralized control of the microgrid through the UDI models.

Note that the above UDI models provide the interfaces among the agents and the controllable devices, and the main characteristics of the agents, such as the autonomy, intelligence, sociality, proactivity, and adaptability, are modeled by heuristic procedures in MATLAB. Using these specific characteristics of the agents, the implemented agents can serve more functionalities than the traditional controls and solve the special needs and difficulties of the proposed decentralized frequency control. The corresponding functionalities the agents serve during the process of the control are described as follows:

1) *Autonomous Local Control:* Use the autonomy of agents to implement the local control autonomously, such as evaluate the corresponding distributed unit and make the classification according to its relative participation during frequency control, as can be seen in Table I; estimate the available power of DGs, as in (10); and calculate the amounts of controllable loads, as in (11).
2) *Proactive Disturbance Response:* Use the proactivity and adaptability of agents to respond to the disturbances, such as monitor the frequency derivation and deal with the data for information sharing, as shown in Fig. 6; implement the multi-stage loads shedding when reserved power is not enough; and meet the requirements for the plug-and-play operations.
3) *Intelligent Cooperative Control:* Use the sociality and cooperation of agents to implement the information sharing and achieve a cooperative frequency recovery, such as perform convergence judgment of the ACA and send control commands back to PSCAD as in (9), (10), and (11).

The lookup table for the network topology in Fig. 6 describes the data of the microgrid for information sharing, which are collected by the agents in a decentralized manner through the UDI models. It is not necessary to store these data in a central agent or a virtual central point, because the data are stored in each agent and exchanged among neighbors. The information exchange for an agent and its immediate neighbors is based on (1), and the data in this equation are all collected by the UDI models from PSCAD in a distributed way. For example, Agent 3, whose neighbor is Agent 1, only needs to exchange data with Agent 1 during the information sharing process. When the convergence judgment of the ACA is reached in each distributed agent, the control reference values are sent back to PSCAD for decentralized control through the UDI models.

A. Simulation Cases

At the beginning of the simulation case, the islanded microgrid works in a well-balanced state. MT works in the VF mode. PV operates in the maximum power point tracking (MPPT) mode, WT operates in the power reserve mode, and SMES and BESs operate in the PQ mode. The total output of DERs is 78 kW, including 38 kW of MT, 30 kW of WT (DFIG), and 10 kW of PV, and the BES is fully charged for power reserves. The total loads are 10 kW of first stage loads, 28 kW of second stage loads, and 40 kW of third stage loads.

Case A: Overload Scenario: When $t = 2$ s, an overload disturbance scenario occurs in the autonomous microgrid, the load in bus 4 changes from 40 to 52 kW; as a result, the power balance between the supply and demand does not match at that moment and the frequency starts to fluctuate.

Case B: Overload Scenario With Plug-In Operation: When $t = 2$ s, an overload scenario occurs in the simulation microgrid with load at bus 4 changing from 40 to 54 kW. At the same time, to enhance the primary frequency control capacity, the BES_2 plugs into the microgrid and is identified as Agent 8, as shown in Fig. 3.

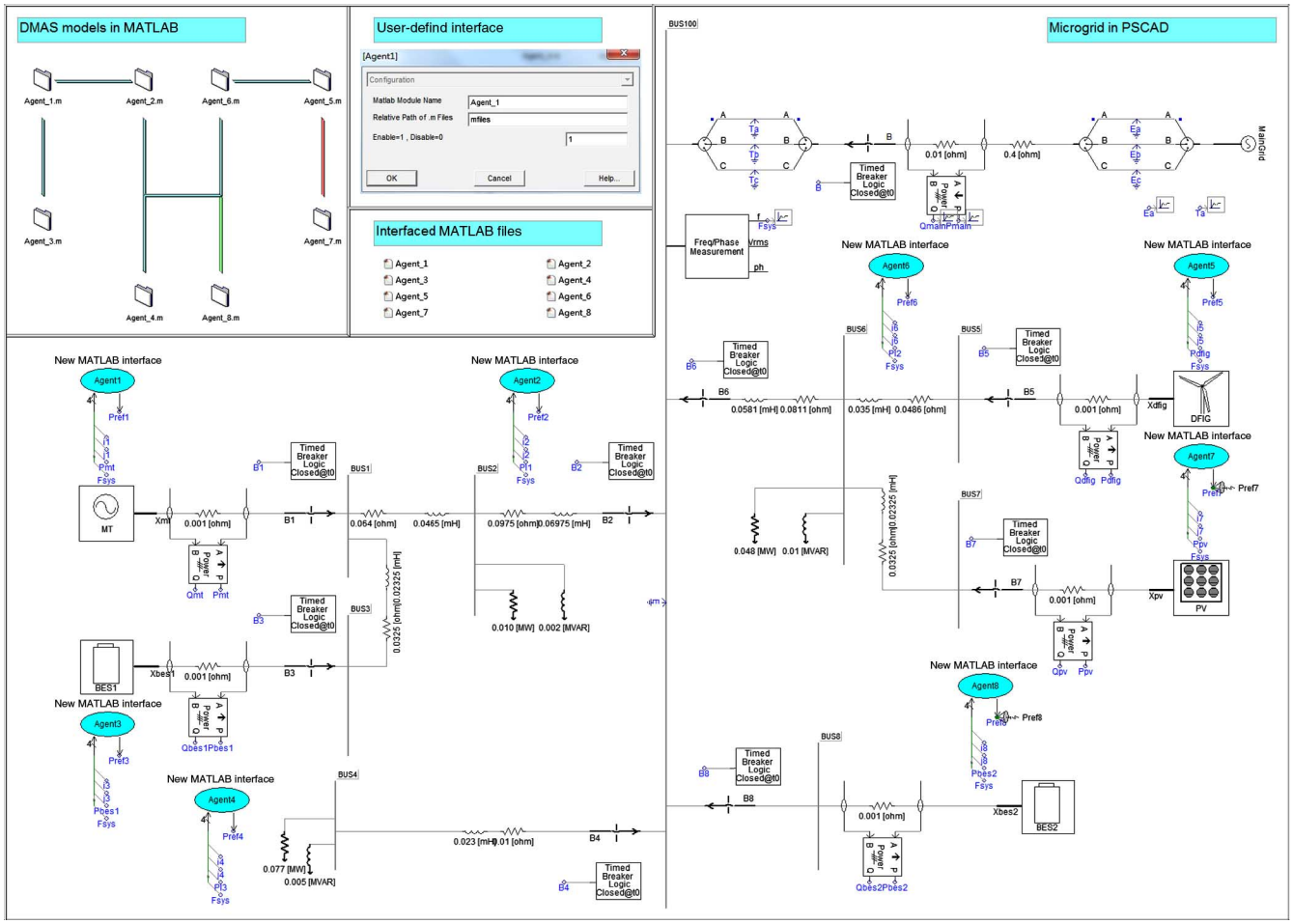

Fig. 5. Simulation models of the DMAS-based microgrid.

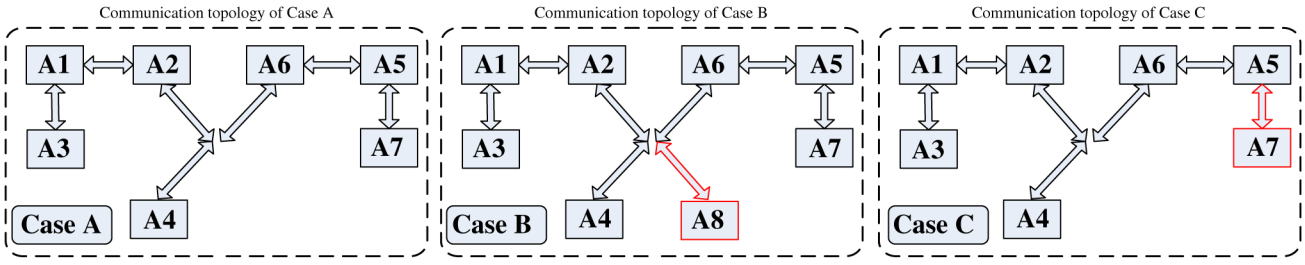

ACA based information sharing of Case A

Agent	Neighbor	Priority	P	P_{DEF}	P_{AVA}	P_{LS}
1	2,3	2	38		27	
2	1,4,6	3	−10			10
3	1	1	0	12		
4	2,6	3	−40			40
5	6,7	2	30		10	
6	2,4,5	3	−28			28
7	5	2	10		0	

ACA based information sharing of Case B

Agent	Neighbor	Priority	P	P_{DEF}	P_{AVA}	P_{LS}
1	2,3	2	38		27	
2	1,4,6 ,8	3	−10			10
3	1	1	0	8		
4	2,6 ,8	3	−40			40
5	6,7	2	30		10	
6	2,4,5 ,8	3	−28			28
7	5	2	10		0	
8	2,4,6	1	0	6		

ACA based information sharing of Case C

Agent	Neighbor	Priority	P	P_{DEF}	P_{AVA}	P_{LS}
1	2,3	2	60		5	
2	1,4,6	3	−10			0*10
3	1	1	0	10		
4	2,6	3	−62			1*62
5	6	2	40		0	
6	2,4,5	3	−38			0.5* 38

Fig. 6. Communication topologies and operation information.

Case C: Overload Scenario With Plug-Out Operation: In this case, MT works in the VF mode and BES_1 operates in the PQ mode. Both DFIG and PV operate in the MPPT mode. The total output of the DERs is 110 kW, including 60 kW of MT, 40 kW of DFIG, and 10 kW of PV, and the BES_1 is fully charged for power reserves. The total loads are 10 kW of first stage loads, 38 kW of second stage loads, and 62 kW of third stage loads.

When $t = 2$ s, the PV bus shuts down because of a fault. Consequently, the power balance and communication topology of the simulation microgrid are both changed because of the plug-out operation.

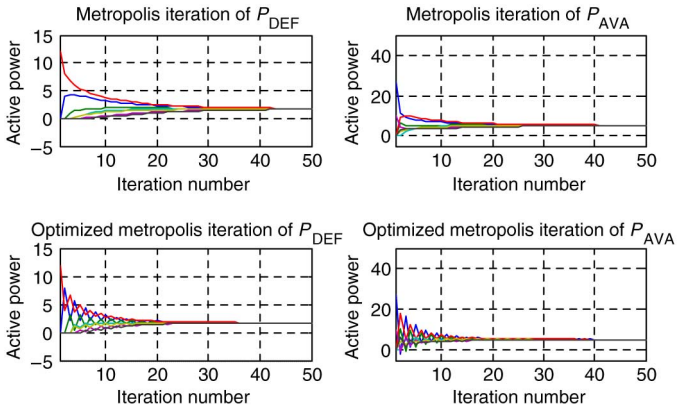

Fig. 7. Comparison of the different updating methods of ACA.

B. Optimized ACA-Based Information Sharing

Fig. 6 illustrates the communication topologies, ID updating process, and local information for sharing in the simulation cases. Based on the communication topologies in Fig. 6, the information exchange coefficient between the neighbors can be determined by (5) for the optimized ACA-based information sharing method. Unlike the communication topologies of the other cases, the coefficient for information exchange between the neighboring agents w, and the numbers of agents that participate in global information sharing n, would change accordingly. According to the above (2), (8), and (11), $P_{\rm DEF}$, $P_{\rm AVA}$, and $P_{\rm LS}$ can then converge to the new average values, respectively. Consequently, the global information of $P_{\rm DEF}^{\rm TOT}$, $P_{\rm AVA}^{\rm TOT}$, and $P_{\rm LS}^{\rm MAX}$ is shared in a distributed way to all decentralized agents for decision making. Finally, based on the shared global information achieved by proposed ACA, the DMAS-based frequency control can be implemented to achieve a cooperative frequency recovery.

C. Convergence of Optimized ACA

In Case A, both the *Metropolis* and the proposed optimized *Metropolis* updating methods of ACA are used for information sharing, the corresponding updating matrix can be set according to (4) and (5), and the information sharing processes are shown in Fig. 7.

It can be observed from Fig. 7 that the proposed method can adapt the plug-and-play operations of the switching topologies as a *Metropolis* method, and converge faster than the *Metropolis* method, with fewer iterations.

The time delay is the key issue for online frequency control of a microgrid. Generally, the time delay consists of the communication and calculation time delays. In this case, the calculation time delay in MATLAB can be ignored, and by setting $n_e = 4$, $n_P = 8$, and $n_{\rm bit} = 16$, the communication time delay under different communication speeds in terms of megabit/seconds can consequently be achieved according to (2) and (7). The time delays of *Metropolis* and the optimized *Metropolis*, for Case A, are calculated and compared in Table II.

It is observed from Table II that the time delays of the optimized *Metropolis* are all smaller than those of *Metropolis*. Based on Fig. 2, according to the flowchart of frequency control for an islanded microgrid, the frequency control is implemented to achieve the cooperative frequency recovery in Case A.

TABLE II
COMPARISON OF TIME DELAYS UNDER DIFFERENT SPEEDS

Network speed	Time delay (s)					
	Metropolis			Optimized metropolis		
	$P_{\rm DEF}$	$P_{\rm AVA}$	Case A	$P_{\rm DEF}$	$P_{\rm AVA}$	Case A
2 Mb/s	0.0098	0.0068	0.0166	0.0061	0.0049	0.0110
4 Mb/s	0.0049	0.0034	0.0083	0.0031	0.0024	0.0055
8 Mb/s	0.0024	0.0017	0.0041	0.0015	0.0012	0.0027
20 Mb/s	0.0010	0.0007	0.0017	0.0006	0.0005	0.0011

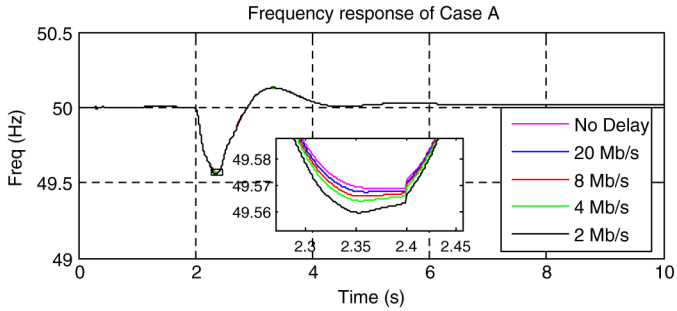

Fig. 8. Optimized ACA-based information sharing.

To test the influence of time delay on frequency control, the frequency control curves of the optimized *Metropolis* in Case A under different network speeds are described and compared, as shown in Fig. 8.

Comparing the frequency control curves in Fig. 8, it is obvious that the influence of time delay on frequency control is small. Even if the communication network speed is 2 Mb/s, the communication time delay in the simulation case is tolerable and can be acceptable for practical online frequency control in an islanded microgrid. About 8 Mb/s is chosen for the analysis in the following simulation cases by coordinating the cost and speed of communication.

D. Case B: Cooperative Frequency Control With Plug-In Operation

Depending on the ACA-based information sharing, both the $P_{\rm DEF}^{\rm TOT}$ and $P_{\rm AVA}^{\rm TOT}$ are shared with all decentralized agents in a distributed manner (and as Step 2 in Fig. 2, the global information is compared as $P_{\rm DEF}^{\rm TOT} < P_{\rm AVA}^{\rm TOT}$), so control decisions can be made to achieve the cooperative frequency control of the microgrid with communication time delay. The iteration processes of the information sharing are described, as shown in Fig. 9.

The time delays for proposed ACA-based information sharing are estimated as 0.0018 and 0.0014 s, respectively, according to Fig. 9, and have little influence on online frequency control.

Three types of strategies including no control, commonly used LS, and DMAS-based frequency control, are separately implemented to verify the validity of the proposed approach. It has to be noted that, because of the communication constraints, the commonly used LS applied in this study can maintain the frequency stability only by cutting the loads adjacent to the

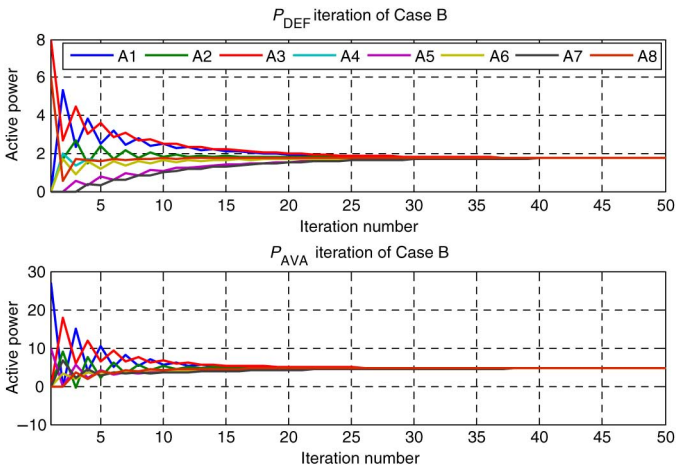

Fig. 9. Global information sharing of Case B.

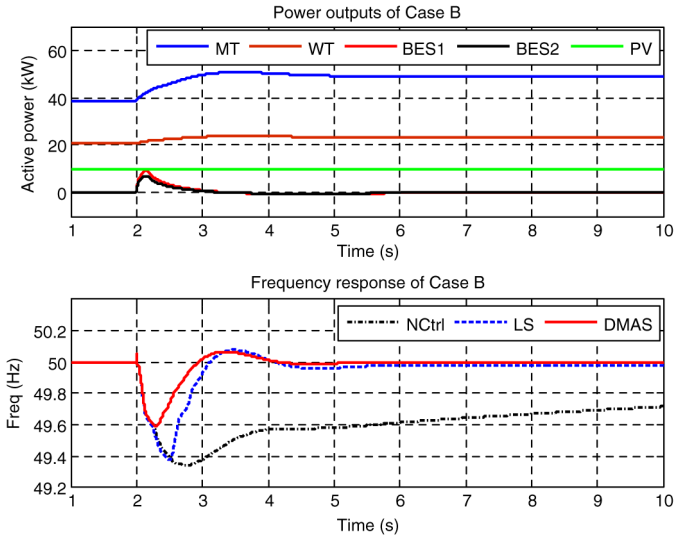

Fig. 10. Cooperative frequency control of Case B.

faulty agent. The power outputs of the microgrid units and the frequency responses are shown in Fig. 10.

From the power output curves of Case B in Fig. 10, it is observed that the quick power change of the ES in primary frequency control is brought back to zero by the power increase of DGs in secondary control. In addition, the power output changes of the MT and WT in the secondary frequency control are both approximately consistent with the power commands calculated from (9).

It is also observed from the frequency response curves of Case B in Fig. 10 that it is necessary to execute LS because the frequency in the dashed line is lower than 49.5 Hz. In the solid line, power deficiency is predicted and offset by the cooperative frequency control strategy with time delay; hence, the corresponding frequency of an islanded microgrid in this case recovers immediately. Compared with the commonly used LS, the frequency quickly becomes higher than 49.5 Hz, which avoids the measurement of LS and decreases the economic cost of operation.

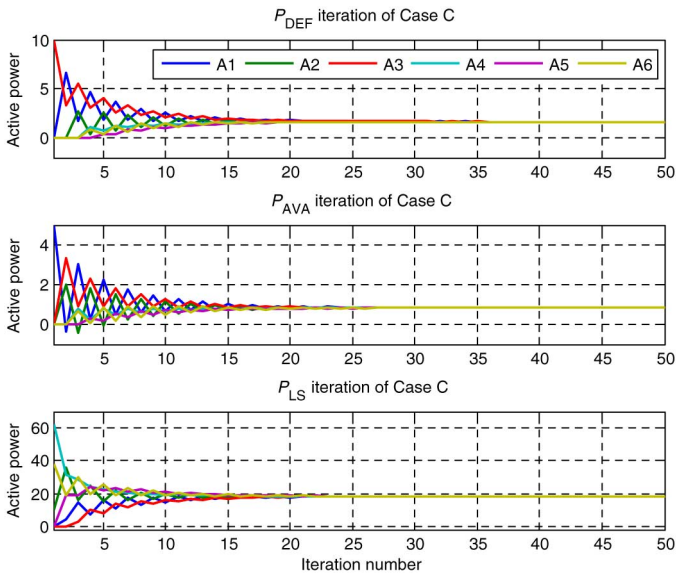

Fig. 11. Global information sharing of Case C.

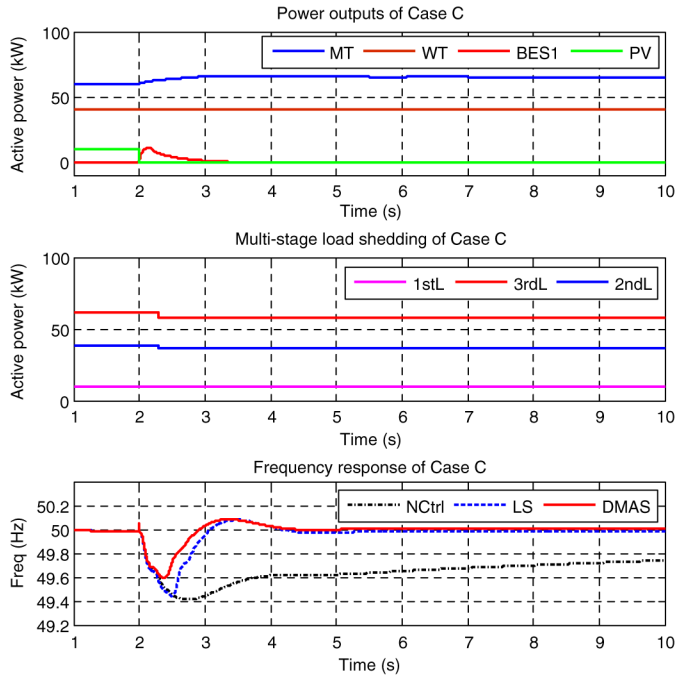

Fig. 12. Cooperative frequency control of Case C.

E. Case C: Cooperative Frequency Control With Plug-Out Operation

According to Step 2 in Fig. 2, the global information, such as $P_{\mathrm{DEF}}^{\mathrm{TOT}}$ and $P_{\mathrm{AVA}}^{\mathrm{TOT}}$, is shared with all decentralized agents in a distributed way based on the proposed ACA information sharing, which is compared as $P_{\mathrm{DEF}}^{\mathrm{TOT}} > P_{\mathrm{AVA}}^{\mathrm{TOT}}$ (10 kW > 5 kW). Therefore, the control decisions are determined by Steps 4 and 5 in Fig. 2, and the other global information $P_{\mathrm{LS}}^{\mathrm{MAX}}$ is discovered as $(n * P_{\mathrm{LS}})$. Accordingly, the LS is implemented based on the discovered global information and the iteration processes of information sharing are shown in Fig. 11.

It is observed in Fig. 11 that the time delays of information sharing, which are 0.0014, 0.0012, and 0.0013 s, have little influence on online frequency control.

In this case, the values of ξ_{Lz} in (11) are set as 0.0, 0.5, and 1.0, which correspond to the first, second, and third stage loads, respectively. Based on (11), the loads to be shed for different stages are distributed as $\Delta P_{L1} = 0$ kW, $\Delta P_{L2} = 1$ kW, and $\Delta P_{L3} = 4$ kW, which are much less than that for commonly used LS (loads are shed adjacent to the faulty agent under communication constraints, 10 kW at bus 6). It can be observed from the curves of the second figure in Fig. 12 that the load changes are in accordance with the power commands distributed by the multi-stage LS strategy. According to the dashed–dotted line of the frequency response in Fig. 12, it is obvious that the frequency of the islanded microgrid cannot recover to 50 Hz because the MT reaches its capacity limit. However in the solid curve, through both the multi-stage LS and power control of the DGs, the frequency was promptly restored to 50 Hz.

VI. Conclusion

A DMAS-based cooperative frequency control scheme for islanded microgrids has been presented and tested in this paper. The simulation results focus on demonstrating the following:

1) The optimized ACA can improve the convergence speed and make the proposed control strategy more adequate for online application; moreover, it is independent of the system configuration, which enables it to meet the requirements for plug-and-play operations of a microgrid.
2) Meanwhile, the DMAS-based cooperative frequency control using decentralized decision making can guarantee the consensus and coordination of distributed agents and effectively enhance the frequency stability of the autonomous microgrid.
3) In addition, the decentralized multi-stage LS can ensure frequency recovery when the power spinning reserve margin is insufficient.

References

[1] N. Pogaku, M. Prodanovic, and T. C. Green, "Modeling, analysis and testing of autonomous operation of an inverter-based microgrid," *IEEE Trans. Power Electron.*, vol. 22, no. 2, pp. 613–625, Mar. 2007.

[2] G. Diaz, C. Gonzalez-Moran, J. Gomez-Aleixandre, and A. Diez, "Complex-valued state matrices for simple representation of large autonomous microgrids supplied by PQ and VF generation," *IEEE Trans. Power Syst.*, vol. 24, no. 4, pp. 1720–1730, Nov. 2009.

[3] J. A. Pecas Lopes, C. L. Moreira, and A. G. Madureira, "Defining control strategies for microgrids islanded operation," *IEEE Trans. Power Syst.*, vol. 21, no. 2, pp. 916–924, May 2006.

[4] F. Katiraei, M. R. Iravani, and P. W. Lehn, "Micro-grid autonomous operation during and subsequent to islanding process," *IEEE Trans. Power Del.*, vol. 20, no. 1, pp. 248–257, Jan. 2005.

[5] A. Oudalov, D. Chartouni, and C. Ohler, "Optimizing a battery energy storage system for primary frequency control," *IEEE Trans. Power Syst.*, vol. 22, no. 3, pp. 1259–1266, Aug. 2007.

[6] A. Tsikalakis and N. Hatzargyriou, "Centralized control for optimizing microgrids operation," *IEEE Trans. Energy Convers.*, vol. 23, no. 1, pp. 241–248, Mar. 2008.

[7] F. Katiraei and M. R. Iravani, "Power management strategies for a microgrid with multiple distributed generation units," *IEEE Trans. Power Syst.*, vol. 21, no. 4, pp. 1821–1831, Nov. 2008.

[8] J. Conroy and R. Watson, "Frequency response capability of full converter wind turbine generators in comparison to conventional generation," *IEEE Trans. Power Syst.*, vol. 23, no. 2, pp. 649–656, May 2008.

[9] M. Chen, L. Yu, N. S. Wade *et al.*, "Investigation on the faulty state of DFIG in a microgrid," *IEEE Trans. Power Electron.*, vol. 26, no. 7, pp. 1913–1919, Jul. 2011.

[10] J. M. Mauricio, A. Marano, E. A. Gomez *et al.*, "Frequency regulation contribution through variable-speed wind energy conversion systems," *IEEE Trans. Power Syst.*, vol. 24, no. 1, pp. 173–180, Feb. 2009.

[11] Y. A. I. Mohamed and A. A. Radwan, "Hierarchical control system for robust microgrid operation and seamless mode transfer in active distribution systems," *IEEE Trans. Smart Grid*, vol. 2, no. 2, pp. 352–362, Jun. 2011.

[12] J. Y. Kim, J. H. Jeon, S. K. Kim *et al.*, "Cooperative control strategy of energy storage system and microsources for stabilizing the microgrid during islanded operation," *IEEE Trans. Power Electron.*, vol. 25, no. 12, pp. 3037–3048, Dec. 2010.

[13] W. Gu, C. Shen, and Z. Wu, "Multi-agent based frequency control of islanded microgrid," *Int. Rev. Electr. Eng.*, vol. 6, no. 7, pp. 3134–3141, Nov. 2011.

[14] W. Gu, W. Liu, C. Shen, and Z. Wu, "Multi-stage underfrequency load shedding for islanded microgrid with equivalent inertia constant analysis," *Int. J. Electr. Power Energy Syst.*, vol. 46, no. 2, pp. 36–39, Mar. 2013.

[15] F. Xiao, L. Wang, and Y. Jia, "Fast information sharing in networks of autonomous agent," in *Proc. Amer. Control Conf.,* 2008, pp. 4388–4393.

[16] Y. Xu and W. Liu, "Novel multiagent based load restoration algorithm for microgrids," *IEEE Trans. Smart Grid*, vol. 2, no. 1, pp. 152–161, Mar. 2011.

[17] L. Xiao, S. Boyd, and S. J. Kim, "Distributed average consensus with least-mean-square deviation," presented at the 17th Int. Symp. Math. Theory Netw. Syst., Kyoto, Japan, Jul. 24–28, 2006.

[18] R. Olfati-Saber and R. M. Murray, "Consensus problems in networks of agents with switching topology and time-delays," *IEEE Trans. Automat. Contr.*, vol. 49, no. 9, pp. 1520–1533, Sep. 2004.

[19] R. Olfati-Saber, "Flocking for multi-agent dynamic systems: Algorithms and theory," *IEEE Trans. Automat. Contr.*, vol. 51, no. 3, pp. 401–420, Mar. 2006.

[20] A. Jadbabaie, J. Lin, and A. S. Morse, "Coordination of groups of mobile autonomous agents using nearest neighbor rules," *IEEE Trans. Automat. Contr.*, vol. 48, no. 6, pp. 988–1001, Jun. 2003.

[21] W. Ren and R. W. Beard, "Consensus seeking in multi-agent systems under dynamically changing interaction topologies," *IEEE Trans. Automat. Contr.*, vol. 50, no. 5, pp. 655–661, May 2005.

[22] G. Wen, Z. Duan, W. Yu, and G. Chen, "Consensus in Multi-Agent systems with communication constraints," *Int. J. Robust Nonlinear Contr.*, vol. 22, no. 2, pp. 170–180, Jan. 2012.

[23] R. Olfati-Saber, J. A. Fax, and R. M. Murray, "Consensus and cooperation in networked multi-agent systems," *Proc. IEEE*, vol. 95, no. 1, pp. 215–233, Jan. 2007.

[24] Y. Xu, W. Liu, and J. Gong, "Stable multi-agent-based load shedding algorithm for power systems," *IEEE Trans. Power Syst.*, vol. 26, no. 4, pp. 2006–2014, Nov. 2011.

[25] Z. Zhang and M.-Y. Chow, "Convergence analysis of the incremental cost consensus algorithm under different communication network topologies in a smart grid," *IEEE Trans. Power Syst.*, vol. 6, no. 7, pp. 3134–3141, Nov. 2011.

[26] M. Pipattanasomporn, H. Feroze, and S. Rahman, "Securing critical loads in a PV-based microgrid with a multi-agent system," *Renew. Energy*, vol. 39, no. 1, pp. 166–174, Mar. 2012.

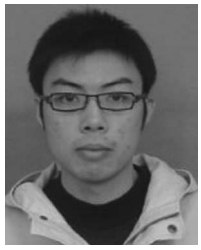

Wei Liu (S'13) received the M.Eng. degree in electrical engineering from Southeast University, Nanjing, China, in 2011. He is currently pursuing the Ph.D. degree in electrical engineering at Southeast University, Nanjing, China.

His research interests are power system stability and control, renewable energy technology, and microgrids.

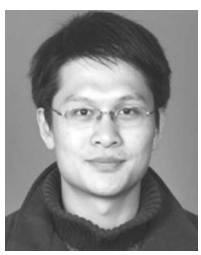

Wei Gu (M'06) received the B.Eng. degree and the Ph.D. degree in electrical engineering from Southeast University, Nanjing, China, in 2001 and 2006, respectively.

He is now an Associate Professor in the School of Electrical Engineering, Southeast University, Nanjing, China. His research interests are power system stability and control, smart grid, renewable energy technology, and power quality.

Wanxing Sheng (M'12) received the B.S., M.S., and Ph.D. degrees from Xi'an Jiaotong University, Xi'an, China, in 1989, 1992, and 1995, respectively.

He is an authorized expert in rural electrical power and distribution network in State Grid Company of China, Beijing, China and a Leader of the Power Distribution Department, China Electrical Power Research Institute, China. Currently, he leads the effort of building smart distribution power system integrated with distributed generators and microgrids throughout China.

Xiaoli Meng (M'12) received the B.S. and M.S. degrees from China Agricultural University, Beijing, China, in 1994 and 2001, respectively.

Currently, she is a Director with the Power Distribution Department, China Electrical Power Research Institute, China. She is now taking the responsibility of smart distribution power system, self-healing control, microgrid modeling and simulation, and demonstration projects implementing.

Zaijun Wu (M'10) received the B.S. degree in electrical engineering from Hefei University of Technology, Hefei, China, in 1996 and the Ph.D. degree in electrical engineering from Southeast University, Nanjing, China, in 2004.

He concentrated his research on protection and control of microgrid, communication system and network in smart substation, analysis, and control of electric power quality.

Wu Chen (S'05–M'12) received the B.S., M.S., and Ph.D. degrees in electrical engineering from the Nanjing University of Aeronautics and Astronautics (NUAA), Nanjing, China, in 2003, 2006, and 2009, respectively.

His main research interests include soft-switching dc/dc converters, inverters, and power electronic system integration.